Electronic Supplementary Material (ESI) for Nanoscale.

The chemistry of nucleation: Unravelling the complex formation mechanism of HfO_2 nanocrystals using *in situ* Pair Distribution Function Analysis

Rasmus S. Christensen,[a] Magnus Kløve,[a] Martin Roelsgaard,[a] Sanna Sommer [a] and Bo B. Iversen[a]*

Table of Contents

1) Overview of datasets for real space analysis

The TS data were transformed into PDFs using the xPDFsuite program.[1] In Table S1, the different datasets are tabulated together with the number of summed data frames prior to the Fourier Transform. Lastly, the values used for the *ad hoc* transformation are provided.

Table S1. Dataset used for PDF analysis and the number of summed framed together with the *ad hoc* transformation values.

Sample	# summed frames	*Ad hoc* parameters
T225	1	Q_{min} = 1.0; Q_{max} = 19.0 R_{poly} = 1.1
T250	1	Q_{min} = 0.5; Q_{max} = 18.0 R_{poly} = 1.1
T300	1	Q_{min} = 1.0; Q_{max} = 19.0 R_{poly} = 1.1
T350	1	Q_{min} = 0.5; Q_{max} = 18.0 R_{poly} = 1.1
T400	1	Q_{min} = 1.0; Q_{max} = 18.0 R_{poly} = 1.15
T450	1	Q_{min} = 0.5; Q_{max} = 18.0 R_{poly} = 1.1
PS1	30	Q_{min} = 1.0; Q_{max} = 20 R_{poly} = 1.1
PS2	30	Q_{min} = 1.21834; Q_{max} = 21 R_{poly} = 1.3887
PS3	90	Q_{min} = 1.0; Q_{max} = 21 R_{poly} = 1.1
PS4	28	Q_{min} = 0.5; Q_{max} = 20 R_{poly} = 1.1
PS5	30	Q_{min} = 1.0; Q_{max} = 21 R_{poly} = 1.1
PS6	30	Q_{min} = 1.0; Q_{max} = 20 R_{poly} = 1.1
T225 (used for SPF)	4	Q_{min} = 1.0; Q_{max} = 19 R_{poly} = 1.38
T250 (used for SPF)	3	Q_{min} = 1.0; Q_{max} = 19 R_{poly} = 1.38
T300 (used for SPF)	3	Q_{min} = 1.25; Q_{max} = 19 R_{poly} = 1.38

2) Temperature profile at P21.1

Figure S2 shows the temperature profile of the heater used for the *in situ* synthesis. The profile is obtained by placing a thermocouple inside the fused silica capillary. From the figure, it is apparent that at low temperature (*e.g.* 200 ˚C) the desired temperature is reached within a few seconds whereas it takes up to 3 min at high temperatures (*e.g.* 450 ˚C).

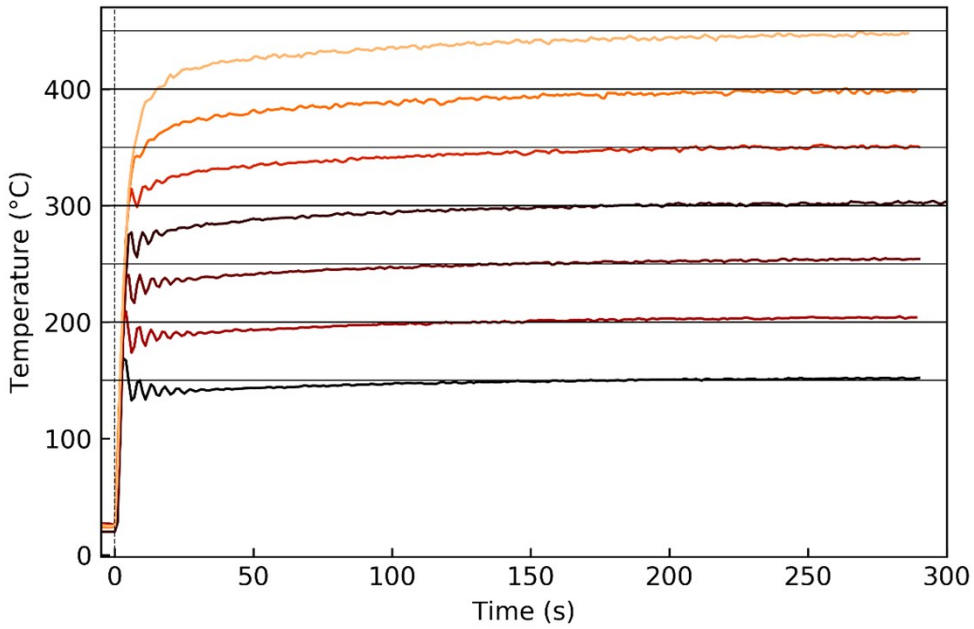

Figure S1. The heating profile of heater used for *in situ* measurements at P21.1.

3) Calibration of detector distance and instrumental resolution

To calibrate the detector distance data were measured on a LaB_6 660b line-broadening standard in a fused silica capillary mounted in the *in situ* setup described by Becker *et al.*[2] The detector distance was calibrated using the Dioptas[3] program and if necessary corrected manually using Python. The manual correction is necessary in some cases where the diffraction rings observed on the detector are not completely circular.

To estimate the instrumental broadening necessary for reciprocal space refinements the LaB_6 diffraction pattern were refined (Figure S1a). Similarly, the PDF of the LaB_6 standard was calculated and refinement in real space (Figure S1b) then yields the dampening of the PDF caused by the instrument. The instrumental dampening is found by refining the Q_{damp} parameter in PDFgui. In this particular experiment, the Q_{damp} parameter were refined to 0.048161.

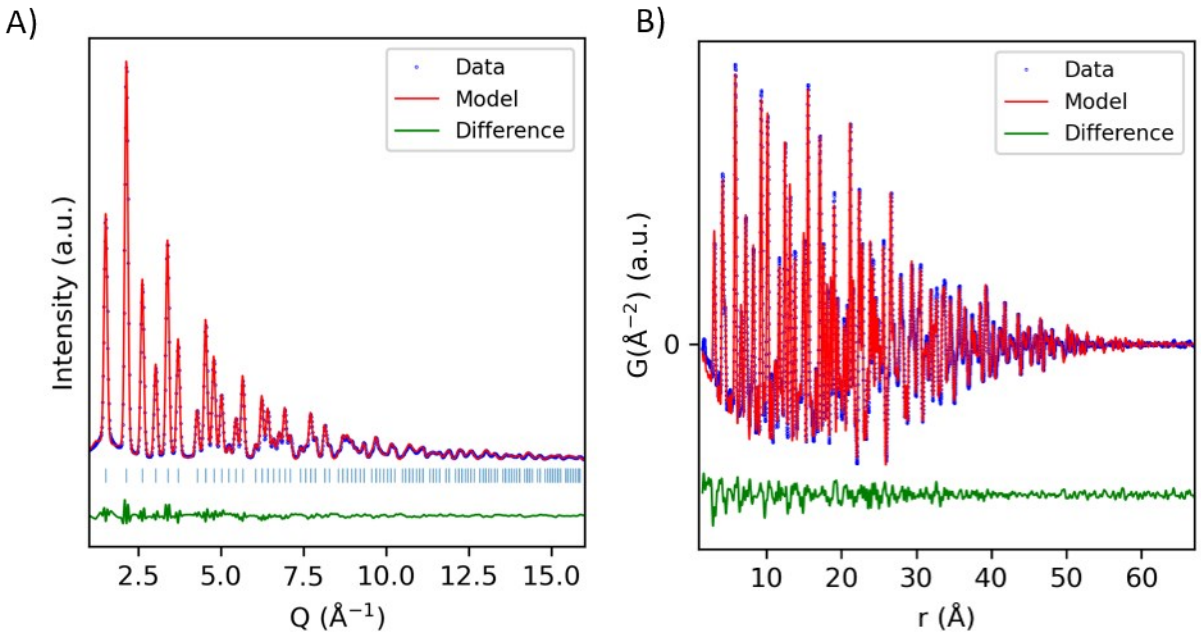

Figure S2. NIST LaB_6 660b line broadening standard refined in a) Reciprocal space, R_{wp} = 3.51, and b) real space, R_w = 0.110.

4) Phase identification

The PDF of the monoclinic (ICSD: 27313)[4], tetragonal(ICSD: 173966)[5] and cubic (ICSD: 173967)[5] HfO_2 structure was simulated and plotted together with the PDF calculated from the final nanocrystal of the T250 data (Figure S3). It is apparent that the obtained particles are predominantly monoclinic. Additional refinements have been done using a two-phase model consisting of *m*- and *t*-HfO_2, however, this refinement showed no trace of *t*-HfO_2.[6]

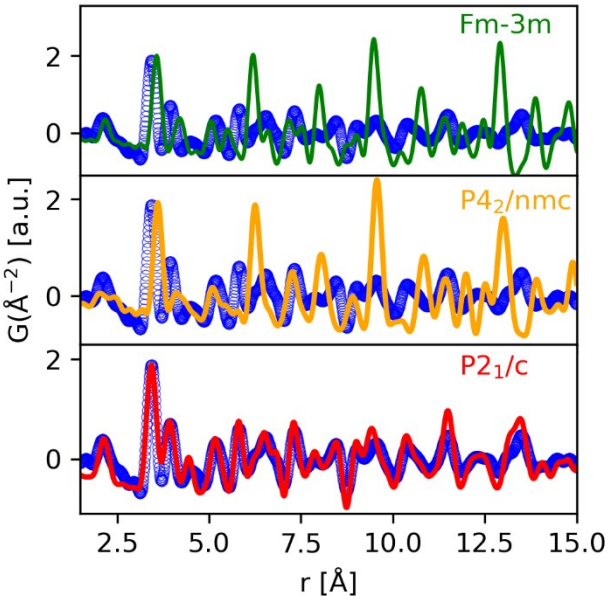

Figure S3. Simulation of PDFs based on *c*-HfO2 (green), *t*-HfO2 (orange) and *m*-HfO2 (red). The blue points are from the final frame of T250.

5) The PS 6 measurement

In Figure 3, five of the six precursor structures are presented. In Figure S11 the PDF of PS 6 is plotted. The PDF shows a large peak at 2.5 Å corresponding to a large amount of Hf-Cl correlations. The PDF also shows a small peak at 3.5 Å indicating that a dimer or trimer structure is observed. It was not possible to obtain a satisfying model for PS 6, however, in order to obtain a relative peak intensity between the Hf-Cl and Hf-Hf correlation of this magnitude the structure must consist of predominantly [$HfCl_x$] monomers.

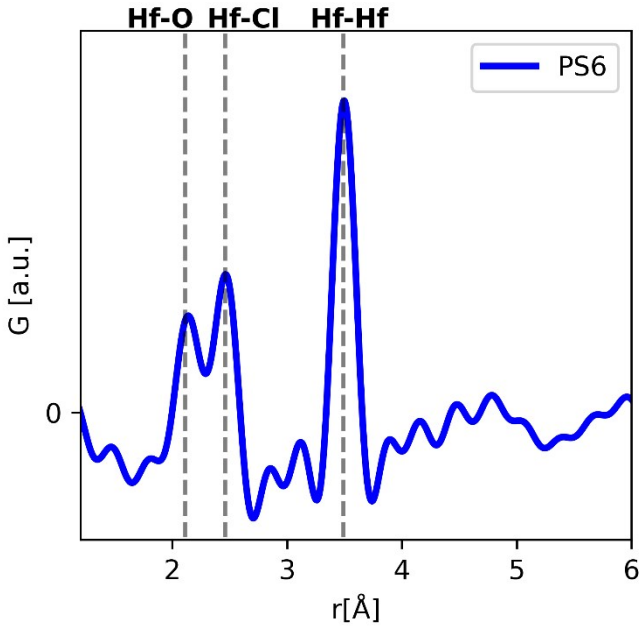

Figure S4. The PDF of PS 6 with the anticipated distances of Hf-O, Hf-Cl and Hf-Hf bond distances marked.

6) Description of sequential refinements

The sequential PDF refinements were done using the PDFgui software.[7] The refinements were done in reverse order, i.e. starting from the last frame and refining backwards towards the first frame. The refined parameters were:

- Scale factor
- Unit cell parameters
- Spherical particle diameter
- Correlated motion
- Isotropic ADP values of Hf and O

The refined values for the unit cell parameters are plotted as a function of the spherical particle diameter in Figure S4.

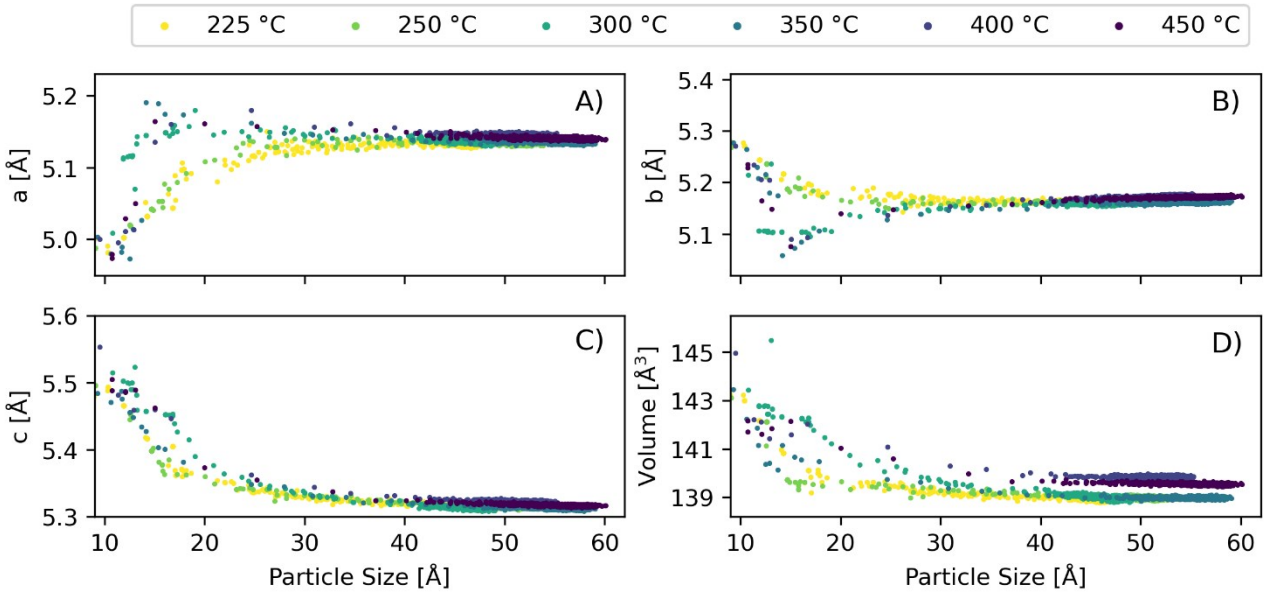

Figure S5. The refined unit cell parameters for T225-450 plotted against the spherical particle diameter.

The Fullprof Suite program package[8] was used in the sequential reciprocal space Rietveld refinements of the *in situ* TS data. Again the refinements were done in reverse order. The refined parameters were

- Scale factor
- Unit cell parameters
- Isotropic ADP values of Hf.
- The size broadening parameter y.

Additionally, the background was modelled in two different ways using either linear interpolated background points or an estimated Chebyshev polynomial. It was found that the best description for T225-T300 was obtained using a Chebyshev polynomial with up to 10 coefficients. However, using a Chebyshev polynomial was not possible for T350-T450, and linear interpolated backgrounds were used instead. The refined values of the final frame are presented in Table S2.

Table S2. The refined parameters of the final frame of each dataset. The values in the white column were obtained from Rietveld refinement and the values in the shaded grey column were obtained from PDF refinements. The literature values were reported by Ruh *et al*.[4]

	225		250		300		350		400		450		Reported
	PXRD						PDF						
a [Å]	5.146 (2)	5.13 (2)	5.143 (2)	5.13 (2)	5.141 (1)	5.13 (2)	5.142 (1)	5.13 (2)	5.152 (2)	5.14 (2)	5.147 (1)	5.14 (2)	5.1126 (5)
b [Å]	5.174 (2)	5.16 (2)	5.174 (2)	5.16 (2)	5.166 (1)	5.16 (2)	5.166 (1)	5.16 (2)	5.178 (1)	5.18 (2)	5.174 (1)	5.17 (2)	5.1722 (5)
c [Å]	5.316 (2)	5.31 (2)	5.317 (2)	5.31 (2)	5.314 (1)	5.31 (2)	5.313 (1)	5.31 (2)	5.323 (1)	5.32 (2)	5.313 (1)	5.32 (2)	5.2948 (5)
β [°]	99.4 (2)	99.6 (3)	99.4 (2)	99.6 (3)	99.0 (2)	99.3 (3)	99.0 (1)	99.3 (3)	98.9 (2)	99.3 (3)	99.0 (1)	99.2 (3)	99.18 (8)
Volume	139.65 (7)	138.6	139.60 (6)	138.6	139.40 (6)	138.7	139.38 (5)	138.7	140.27 (7)	139.8	139.78 (3)	139.6	138.22
U_{iso}(Hf) [Å^2]	0.0033 (4)	0.0075	0.0030 (3)	0.0069	0.0042 (3)	0.0073	0.0044 (3)	0.0079	0.0041 (4)	0.0085	0.0049 (2)	0.0086	0.0057
U_{iso}(O) [Å^2]	NA	0.11	NA	0.12	NA	0.090	NA	0.076	NA	0.074	NA	0.066	0.0057
Delta2	NA	1.8 (3)		1.9 (4)		1.8 (5)		1.8 (6)		1.6 (7)		1.6 (8)	
R_{WP}/R_W	10.3	22.9	9.72	21.0	8.02	19.4	8.17	22.9	9.97	16.0	5.49	15.8	

7) Initial precursor simulations and refinements

The precursor structure has been modelled using four different structures, three of which are dimers while the last is a trimer with equally spaced Hf-atoms. The structures are shown in Figure S5. The models in Figure S5a and c are based on the *m*-HfO_2 crystal structure, whereas the two other models were constructed in order to examine the coordination number of the dimer.

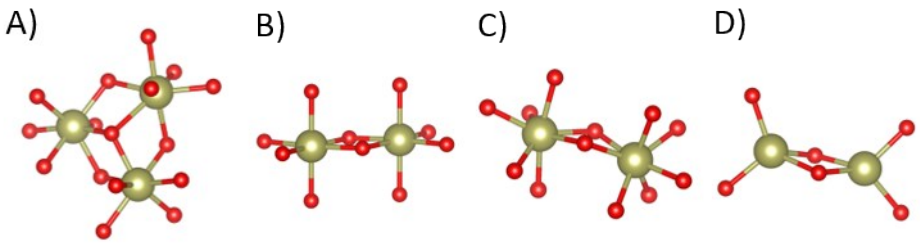

Figure S6. The four different precursor models examined. Red: Oxygen and Gold: Hafnium.

The analysis was made on for the TS data of PS2 as this measurement show a clear separation of all measured peaks. Figure S6-9 shows several refinements where only the scale factor is refined.

The number of substituted chlorine atoms is increased for each model to investigate the relative ratio between the peaks. When evaluating the R_w values plotted in each figure it is clear that the trimer on average gives the best fit of the data. All of these structures display the correct distances, however, the ratio between the peaks are different. The intensity difference between the Hf-O and Hf-Hf correlation is large due to the very sharp peak shape of the Hf-Hf correlation indicating that the hafnium atoms are equally spaced and with low thermal vibration.

Several structures fit the data well when refining multiple parameters due to the quality of the TS data. However, to avoid overparameterization the models are kept simple and with a minimum of refined parameters. In Figure S10 two structures are shown having a good description of the data. The parameter refined in these refinements were the ADP-values of the hafnium atoms in the dimer/trimer structure. The figure illustrates the importance of the ADPs of the hafnium atom as this allows for a significantly better description of the data.

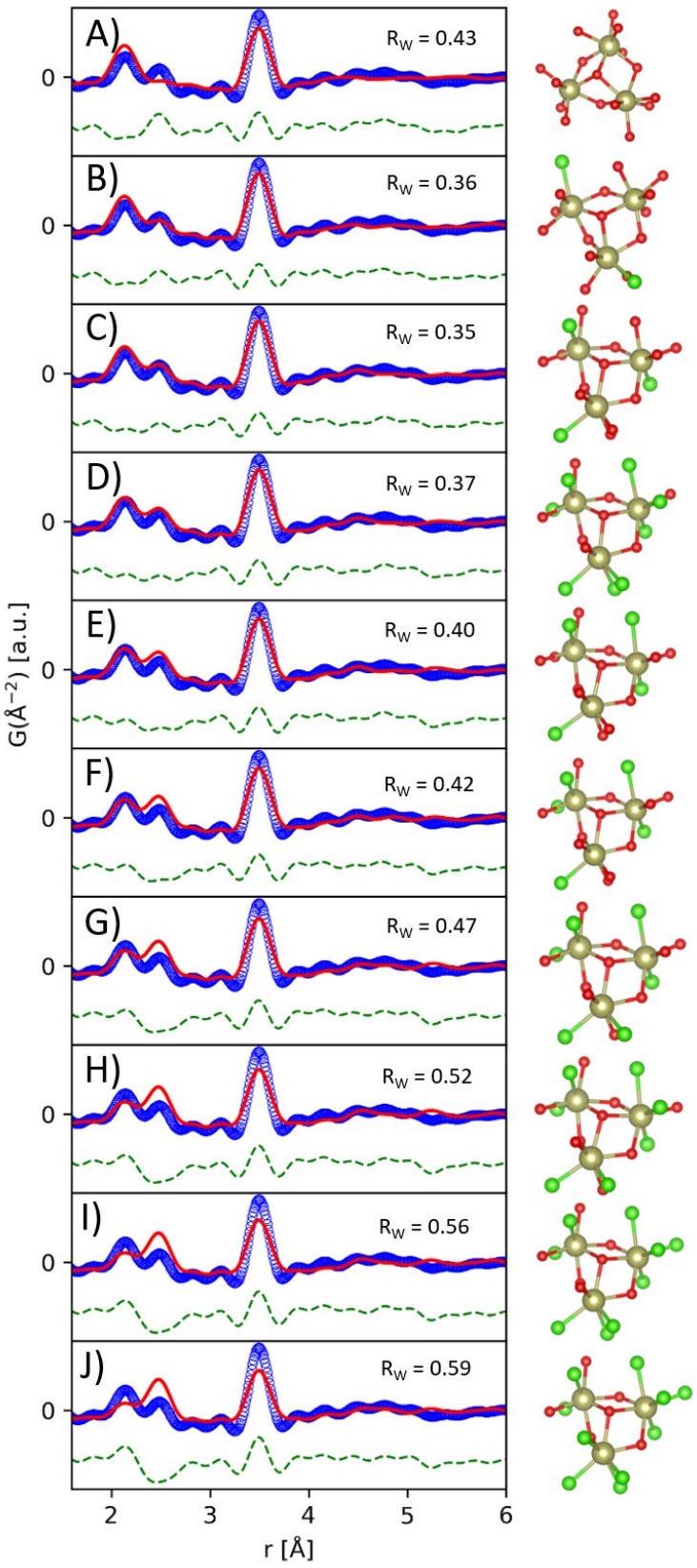

Figure S7. The refined structures of the trimer precursor structure with different amount of substituted chlorine atoms. Red: Oxygen, Gold: Hafnium and Green: Chlorine.

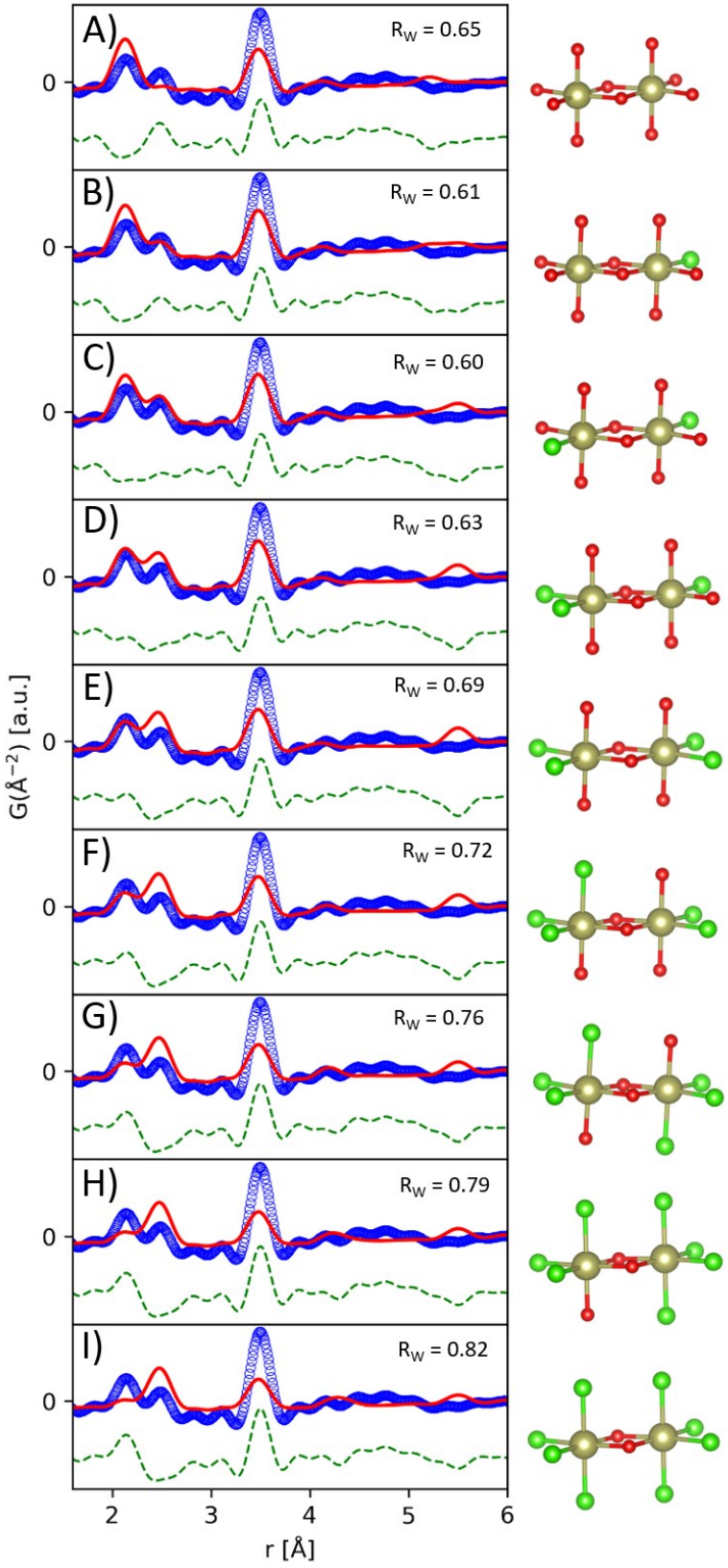

Figure S8. The refined structures of. the octahedrally coordinated dimer with different amount of substituted chlorine atoms. Red: Oxygen, Gold: Hafnium and Green: Chlorine.

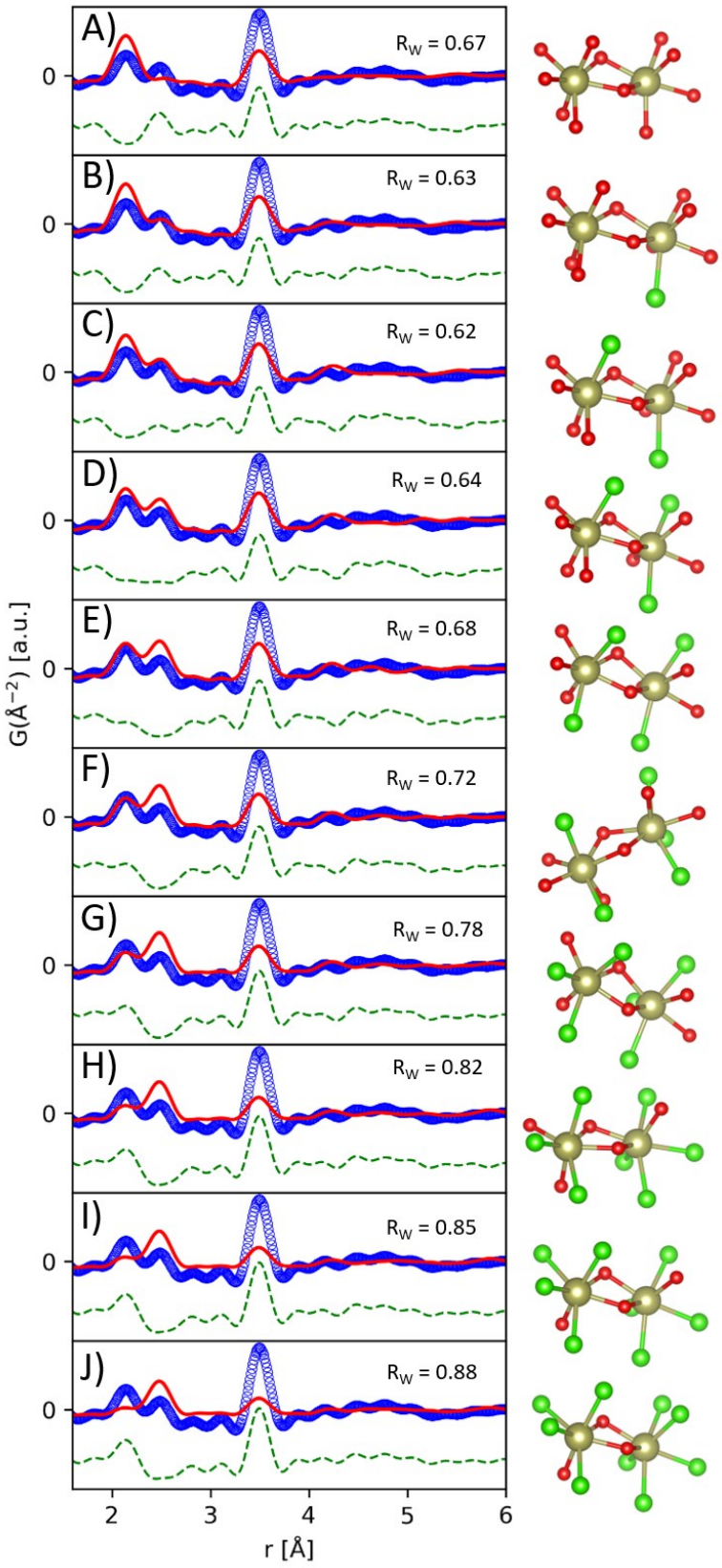

Figure S9. The refined structures of the seven-fold coordinated dimer with different amount of substituted chlorine atoms. Red: Oxygen, Gold: Hafnium and Green: Chlorine.

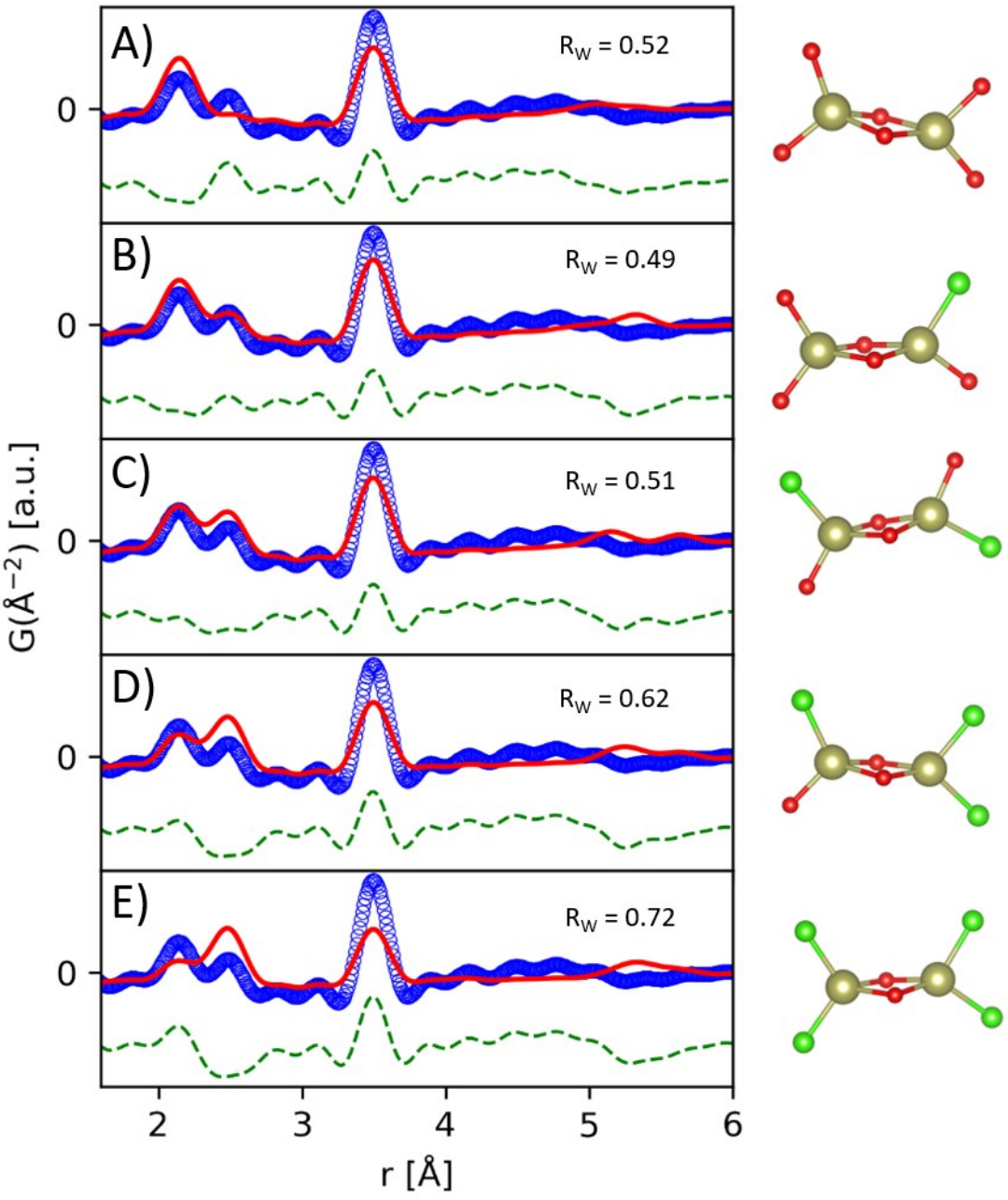

Figure S10. The refined structures of the tetrahedrally coordinated dimer with different amount of substituted chlorine atoms. Red: Oxygen, Gold: Hafnium and Green: Chlorine.

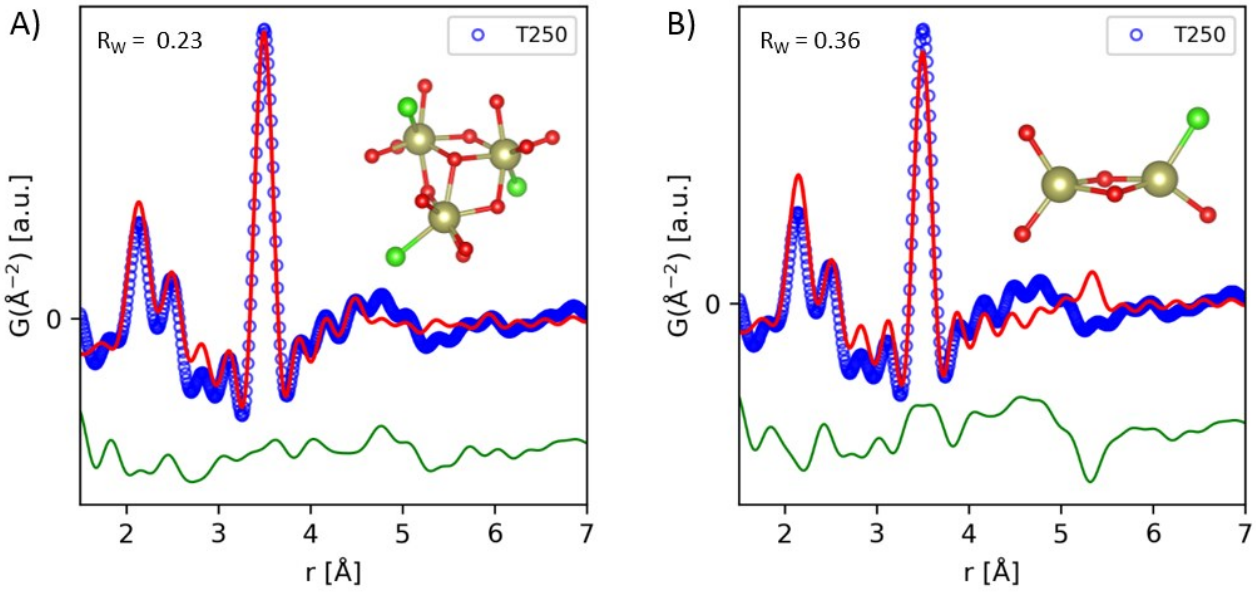

Figure S11. Refinement of T250 precursor data, in which only the ADPs of the Hf-atoms and the scale factor were refined. a) The trimer model. b) The dimer model. Red: Oxygen, Gold: Hafnium and Green: Chlorine.

8) Best refinement of precursor structure

The refinements shown in Figure 3 were calculated refining the scale factor, the ADPs of hafnium and zoomscale. The values are tabulated in Table S3 together with the estimated standard deviation calculated by DiffPy CMI. The zoomscale values are within 5 % of the original model, which indicates that no severe distortions were necessary to obtain the fit.

Table S3. Refined values of the best model of the precursor structure for each of the measurements.

	PS1	PS2	PS3	PS4	PS5
U_{iso}(Hf) [Å^2]	$1 \cdot 10^{-4} \pm 6 \cdot 10^{-10}$	$1 \cdot 10^{-3} \pm 5 \cdot 10^{-3}$	$2 \cdot 10^{-3} \pm 4 \cdot 10^{-3}$	$4 \cdot 10^{-3} \pm 8 \cdot 10^{-3}$	$0.4 \cdot 10^{-3} \pm 5 \cdot 10^{-3}$
Zoomscale a	0.96 (2)	0.97 (6)	0.97 (5)	0.9 (1)	0.96 (7)
Zoomscale b	1.04 (2)	1.00 (9)	1.01 (6)	1.09 (7)	1.05 (4)
Zoomscale c	1.02 (4)	1.04 (8)	1.02 (8)	0.9 (1)	0.98 (9)

9) Initial structural change

As heat is applied to the precursor the Hf-Cl correlations disappears (Figure S12). The peaks at 2.1 and 3.5 Å are preserved, but the peak at 2.5 changes drastically within the first 16 seconds of the experiment. The peak at 2.5 Å increases quickly before it disappears completely. The peak position of 2.5 Å corresponds to the Hf-Cl correlation and the fact that it disappears corresponds well with the fact that the remaining Hf-Cl bonds are eliminated forming additional HCl. The increase in the peak just as heat is applied could be due to the increased motion caused by the rapid heating.

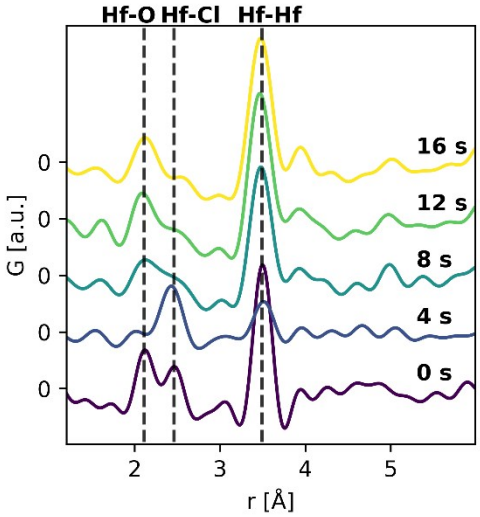

Figure S12. The initial change in the PDFs of sample T250 for the first 16 seconds. The PDFs are plotted with an offset of 0.5.

10) Analysis of the final growth mechanism

A line was fitted to the size obtained from PDF refinements at the point where the growth rate is low (Figure 7). It is expected that the slope of the line will increase with increasing temperature due to increased Ostwald ripening,[12] however as is shown in Figure S14 no clear trend is observed with increasing temperature.

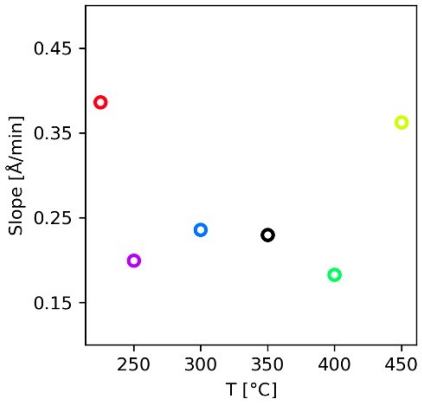

Figure S13. The calculated slopes of the linear fit obtained from the growth curves at the point where the growth rate is low. The colours correspond to the different samples: T225 (Red), T250 (Purple), T300 (Blue), T350 (Black), T400 (Green) and T450 (Yellow).

11) Kinetic analysis using Johnson-Mehl-Avrami

The kinetics of the reaction of $HfCl_4$ in MeOH to form HfO_2 were analysed using the function shown in eq. 10.1, where α is the extent of reaction, k is related to the rate constant and n, is a constant related to the reaction mechanism.

$$\alpha = 1 - \exp\left(-k(t - t_0)^n\right) \qquad 10.1$$

The equation was developed almost simultaneously by Johnson and Mehl and by Avrami, subsequently.[9,10] The theory is considered a classical method of analysing reaction kinetics for solid-state chemical reactions. If the value of n is in the range of 0.54-0.62, then this typically corresponds to a diffusion limited reaction mechanism, 1.0-1.24 corresponds to a zero-order, first-order or phase-boundary-controlled mechanism and 2.0-3.0 corresponds to a nucleation and growth-controlled mechanism. The fitted function and the obtained k and n values are shown in Figure S13. The extent of reaction was estimated as $V(t)/V_{inf}$ where V_{inf} is the final stable nanocrystal volume. The nanocrystallites are assumed spherical in morphology as was reported previously by Buha *et al*. When considering the fits of sample T225 and T250 in Figure S13a and b, it is clear that the function does not describe the data well. For sample T300 – 450 the trend is described by the JMA model, but the obtained n values fall outside the theoretically predicted values. This analysis has previously been used to estimate an activation energy (E_a) of solvothermal synthesis.[11] E_a can be calculated using the Arrhenius equation, $k = A\exp(E_a/RT)$, and is obtained as the slope when ln(k) is plotted vs 1000/T.

However, the obtained k values do not give a linear trend with temperature making estimation of E_a impossible.

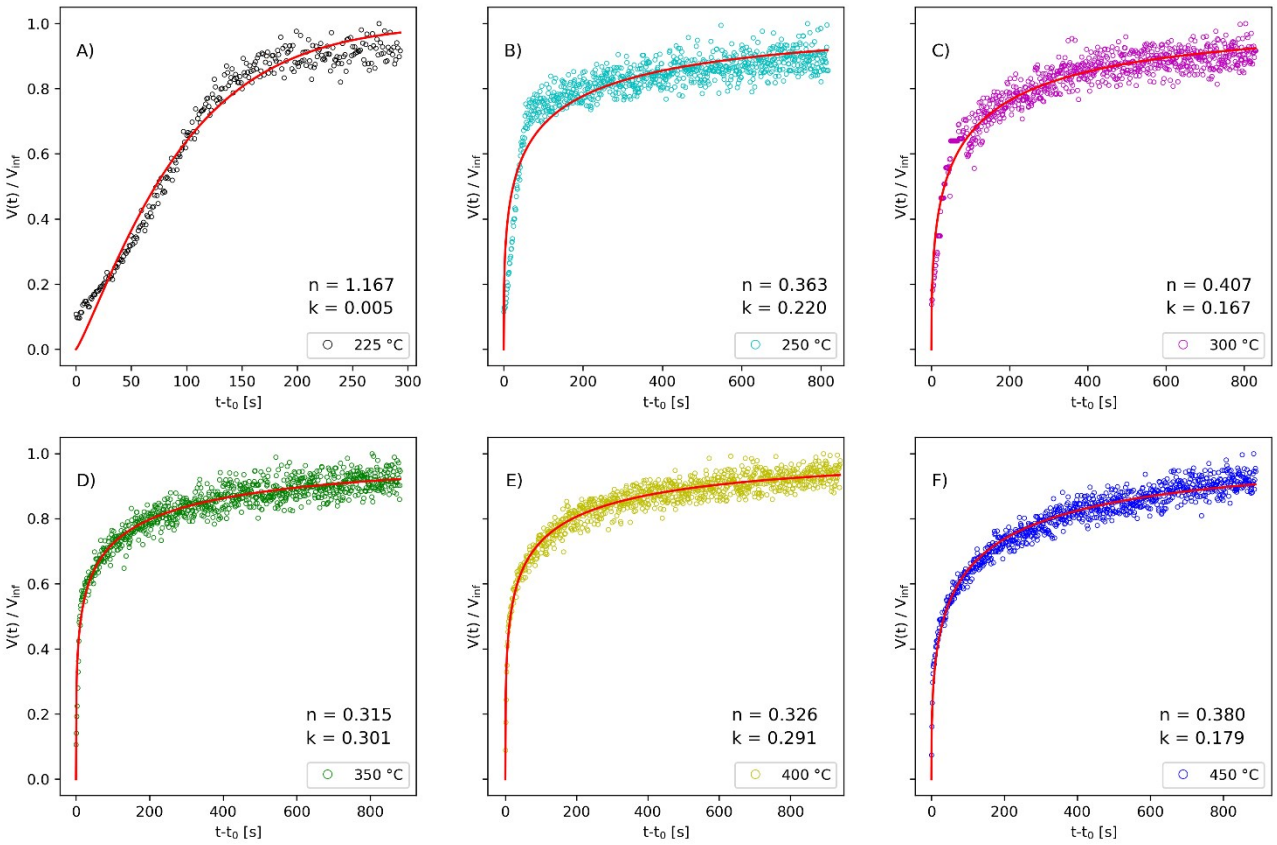

Figure S14. The JMA-function fitted to the extent of reaction. The model was fitted with $V(t)/V_{inf} > 0.1$. The obtained n and k constants are expressed explicitly in each plot.

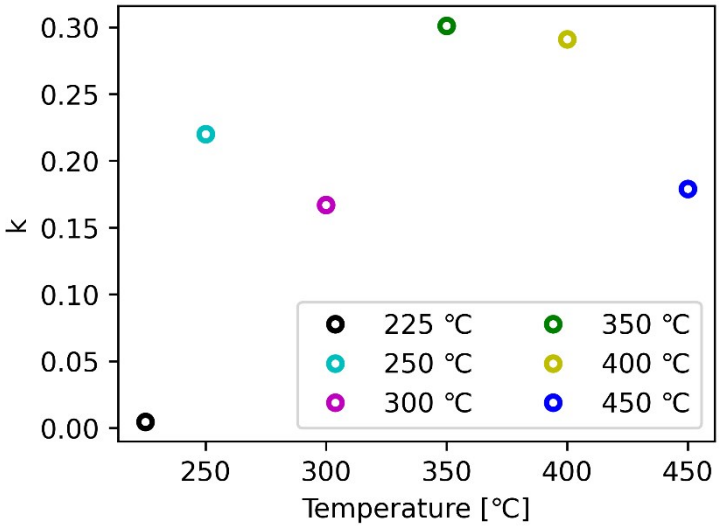

Figure S15. The rate constants, *k*, obtained from the JMA analysis plotted as a function of temperature.

References

1 X. Yang, P. Juhas, C. L. Farrow and S. J. L. Billinge, 2014, 1–4.

2 J. Becker, M. Bremholm, C. Tyrsted, B. Pauw, K. M. O. Jensen, J. Eltzholt, M. Christensen and B. B. Iversen, *J. Appl. Crystallogr.*, 2010, **43**, 729–736.

3 C. Prescher and V. B. Prakapenka, *High Press. Res.*, 2015, **35**, 223–230.

4 R. RUH and P. W. R. CORFIELD, *J. Am. Ceram. Soc.*, 1970, **53**, 126–129.

5 J. E. Jaffe, R. Bachorz and M. Gutowski, *Phys. Rev. B*, 2005, **72**, 144107.

6 R. S. Christensen, Aarhus University, 2019.

7 C. L. Farrow, P. Juhas, J. W. Liu, D. Bryndin, E. S. Boin, J. Bloch, T. Proffen and S. J. L. Billinge, *J. Phys. Condens. Matter*, , DOI:10.1088/0953-8984/19/33/335219.

8 J. Rodríguez-Carvajal, *Phys. B Phys. Condens. Matter*, 1993, **192**, 55–69.

9 W. A. and M. R. F. Johnson, 1939, 135, 416.

10 M. Avrami, *J. Chem. Phys.*, 1939, **7**, 1103–1112.

11 P. Nørby, M. Roelsgaard, M. Søndergaard and B. B. Iversen, *Cryst. Growth Des.*, 2016, **16**, 834–841.

12 I. M. Lifshitz and V. V Slyozov, *J. Phys. Chem. Solids*, 1961, **19**, 35–50.